ANTIOXIDANTS & REDOX SIGNALING
Volume 16, Number 10, 2012

DOI: 10.1089/ars.2011.4504

Does Hyperoxia Selection Cause Adaptive Alterations of Mitochondrial Electron Transport Chain Activity Leading to a Reduction of Superoxide Production?

Huiwen W. Zhao,[1] Sameh S. Ali,[2] and Gabriel G. Haddad[1,3,4]

Abstract

Prolonged hyperoxia exposure generates excessive reactive oxygen species (ROS) and potentially leads to oxidative injury in every organ. We have previously generated *Drosophila melanogaster* flies that tolerate extreme oxidative stress (90%–95% O_2), a lethal condition to naive flies, through a long-term laboratory selection. We found that hyperoxia-selected ($S_{O2}A$) flies had a significantly longer lifespan in hyperoxia and paraquat-induced oxidative stress. Prolonged hyperoxia exposure induced a significant ROS accumulation and an increased expression of oxidative stress markers, including lipid peroxidation and protein carbonyl contents in control flies, but not in $S_{O2}A$ flies. Enzymatic assays revealed that antioxidant enzyme activity in $S_{O2}A$ flies was similar to that in control flies. However, in isolated mitochondria and using electron paramagnetic resonance, we observed that $S_{O2}A$ flies displayed a decreased superoxide yield during state 3 respiration as compared to control flies and that the activity of electron transport chain complex I and III was also inhibited in $S_{O2}A$ flies. Our observations lead to the hypothesis that decreased complex activity results in a decreased ROS production, which might be a major potential adaptive mechanism of hyperoxia tolerance. *Antioxid. Redox Signal*. 16, 1071–1076.

Hyperoxia-Induced Oxidative Stress and Redox Homeostasis

MECHANICAL VENTILATION with high concentration of oxygen (hyperoxia) is essential for patients with difficulties in maintaining adequate oxygenation, but prolonged exposure to hyperoxia generates excessive reactive oxygen species (ROS) and potentially induces oxidant injury in every organ. Despite the fact that numerous studies have defined the phenotype of hyperoxia-induced injury, the mechanisms underlying tissue susceptibility/tolerance to hyperoxia-induced oxidative stress remain elusive.

The balance between antioxidant defense system and free radical production is fundamental for tolerance or susceptibility. Prolonged exposure to hyperoxia induces excessive ROS accumulation, which overwhelms the capacity of endogenous antioxidant defense systems that are designed to preserve normal cellular functions. This may induce oxidative stress as evidenced by an increased lipid peroxidation, protein carbonyl accumulation, and deoxyribonucleic acid (DNA) fragmentation. Clerch and Massaro have shown that increasing manganese superoxide dismutase (MnSOD) activity and stability play an important role in endotoxin-mediated hyperoxia tolerance in lung tissue of adult rats (4). Furthermore, Campian *et al*. suggested that hyperoxia tolerance observed in HeLa-80 cells, as compared to HeLa-20 cells, is due to a decreased ROS production through modification of cytochrome C oxidase activity and a tighter coupling of the electron transport chain (ETC) (2). Therefore, maintaining redox homeostasis by regulation antioxidant defense system or ROS production is one of key mechanisms for tissues to adapt to hyperoxia-induced oxidative stress.

Innovation

The role of mitochondrial electron transport chain (ETC) activity in oxidative stress is controversial. By investigating mechanisms underlying tissue susceptibility/tolerance to hyperoxia-induced oxidative stress and using hyperoxia-selected flies as a model system, this study describes a decreased ROS production combined with a decreased ETC complex activity in these hyperoxia-selected flies and concludes with the hypothesis that decreased ETC complex activity results in a decreased ROS production. We believe that the role that the ETC plays in oxidative stress is likely to be a major potential adaptive mechanism of hyperoxia tolerance and the findings of this work provide experimental evidence for this idea.

Departments of [1]Pediatrics, [2]Medicine and Anesthesiology, and [3]Neuroscience, University of California–San Diego, La Jolla, California.
[4]The Rady Children's Hospital–San Diego, San Diego, California.

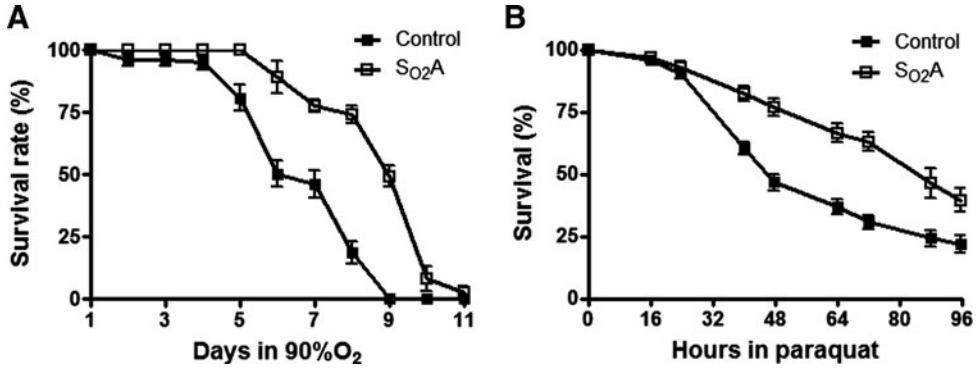

FIG. 1. Prolonged lifespan in oxidative stress. (A) Three- to five-day-old adult flies were exposed to 90% O_2 and percent survival was scored daily. Adult hyperoxia selected ($S_{O2}A$) flies exhibited a significantly better survival in 90% O_2 as compared to control flies and a 25% increase in median and maximum lifespan respectively ($p < 0.01$). **(B)** Three- to five-day-old adult flies were exposed to 15 m*M* paraquat and percent survival was scored every 8–16 h. A greater survival rate was observed in adult $S_{O2}A$ flies as compared to control flies (86% *vs*. 46%) after 48 h of paraquat treatment ($p < 0.01$).

Prolonged Lifespan Under Oxidative Stress

Our laboratory has previously generated *Drosophila melanogaster* flies that tolerate extreme oxidative stress (90%–95% O_2), a lethal condition for naive flies, through a long-term laboratory selection over many generations (8, 9). In the current study, we are using this unique *Drosophila* model to investigate the molecular basis of hyperoxia tolerance. The most striking difference between these hyperoxia-selected ($S_{O2}A$) flies and control flies is that embryos from these $S_{O2}A$ flies were able to complete their life cycle, develop to adult stage, and reproduce indefinitely in 90%–95% O_2. In contrast, embryos from the control population stopped development in 80% O_2 at the first instar larval stage, failed to molt, became necrotic, and died. Although it is well accepted that hyperoxia induces oxidative stress and reduces adult lifespan, adult $S_{O2}A$ flies exhibited a significantly better survival in 90%–95% O_2 as compared to control flies and a 25% increase in median and maximum lifespan respectively (Fig. 1A, $p < 0.01$). Similarly, when we exposed adult $S_{O2}A$ flies to paraquat, a non-selective herbicide that generates free radicals and induces oxidative stress *in vivo*, a greater survival rate was observed in adult $S_{O2}A$ flies than in control flies (86% *vs*. 46%) after 48 h of paraquat treatment (Fig. 1B, $p < 0.01$), suggesting that $S_{O2}A$ flies display tolerance to a broad-spectrum oxidative stress and not only to hyperoxia.

No Evidence of Oxidative Injury Under Hyperoxia

Hyperoxia induces excessive ROS production and causes oxidative stress both *in vivo* and *in vitro*. To examine whether $S_{O2}A$ flies that were perpetually living in hyperoxia exhibited an increased ROS accumulation and oxidative stress injury, we first determined the level of hydrogen peroxide (H_2O_2) in

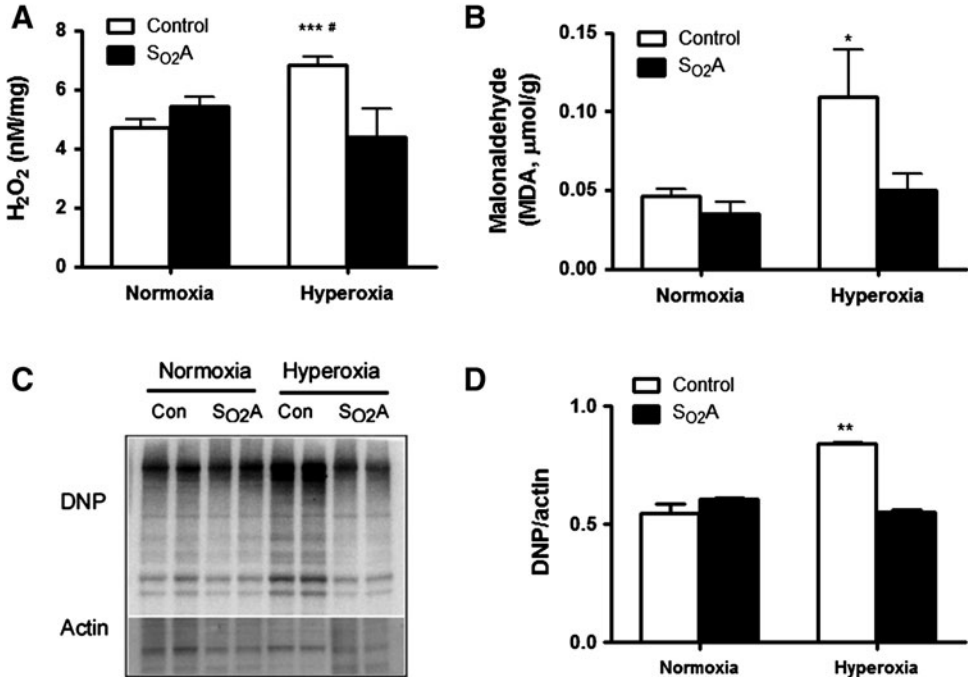

FIG. 2. No evidence of oxidative stress in $S_{O2}A$ flies. (A) The levels of hydrogen peroxide (H_2O_2) in whole tissue homogenate were compared between control flies and $S_{O2}A$ flies. The H_2O_2 level was similar between the two groups in normoxia ($p > 0.05$), but 3 days of hyperoxia treatment significantly increased H_2O_2 level in control flies ($p < 0.001$) but not in $S_{O2}A$ flies. Three days of hyperoxia treatment also significantly increased the accumulation of **(B)** malonaldehyde (MDA) ($p < 0.05$) and **(C, D)** 2,4-dinitrophenylhydrazine (DNP) ($p < 0.01$) in control flies, but not in $S_{O2}A$ flies. $^{*}p < 0.05$, $^{**}p < 0.01$, and $^{***}p < 0.001$; $^{\#}p < 0.05$ when compared with $S_{O2}A$ flies in hyperoxia.

$S_{O2}A$ flies and control flies in normoxia and hyperoxia. As shown in Figure 2A, the levels of H_2O_2 were similar in control and $S_{O2}A$ flies in normoxia (Fig. 2A, $p > 0.05$). However, there was a major difference between control and $S_{O2}A$ flies in hyperoxia; control flies increased their H_2O_2 level over that in normoxia after 3 days of hyperoxia treatment (Fig. 2A, $p < 0.001$), but $S_{O2}A$ flies did not.

Next, we measured the level of malonaldehyde (MDA) and 2,4-dinitrophenylhydrazine (DNP), markers of lipid peroxidation and protein oxidation, respectively. Consistent with the H_2O_2 results, we observed that 3 days of hyperoxia in control flies significantly increased the accumulation of MDA (Fig. 2B, $p < 0.05$) and DNP (Fig. 2C, D, $p < 0.01$). However, the level of MDA and DNP was not increased when $S_{O2}A$ flies were exposed to the same hyperoxia level ($p > 0.05$).

These data led us to ask why hyperoxia did not induce oxidative injury in $S_{O2}A$ flies that have been living in 90%–95% O_2 over many generations. One possible explanation is that hyperoxia treatment induces ROS production in $S_{O2}A$ flies, but also an increased antioxidant defense capacity in $S_{O2}A$ flies to naturalize the hyperoxia-induced stress responses. Another possible explanation is that hyperoxia exposure does not induce an increased ROS production in $S_{O2}A$ flies, so these flies do not sense oxidative stress at all.

Similar Antioxidant Enzyme Activity Between Control and $S_{O2}A$ Flies

The effect of hyperoxia on antioxidant enzyme activity has been reported previously. For instance, 90 min of hyperoxia significantly decreased SOD activity in the lung of Wistar rats. A longer period, such as 60 h, of hyperoxia can induce an increased MnSOD activity in brain mitochondria of guinea pigs. Furthermore, the MnSOD activity was significantly higher than that in normoxia in macrophage culture after 3 weeks of intermittent hyperoxia. These data demonstrate that the effect of hyperoxia on antioxidant enzyme activity is varied and based on the duration of treatment. Increased SOD activity has been shown to attenuate hyperoxia-induced oxidative injury in A549 cells and in dopaminergic neurons, demonstrating that increased antioxidant enzyme activity can act as a protective mechanism against hyperoxia-induced injury.

To examine whether enhanced hyperoxia tolerance was due to an increased antioxidant buffering capacity (*e.g.*, antioxidant enzyme activity), we first measured enzyme activities of SOD, catalase, and peroxidase. As shown in Figure 3, no difference was observed in the activities of catalase (Fig. 3A), peroxidase (Fig. 3B) and MnSOD (Fig. 3C) between control flies and $S_{O2}A$ flies ($p > 0.05$), indicating that $S_{O2}A$ flies do not rely on an increased antioxidant enzyme activity to protect themselves from hyperoxia-induced oxidative stress or a time-dependent change in antioxidant enzyme activity is not detected. However, we found a significantly decreased copper and zinc SOD (CuZnSOD) activity in $S_{O2}A$ flies as compared to control flies (Fig. 3C, $p < 0.01$). Since CuZnSOD is located in the cytosol and intermembrane space of mitochondria, a decreased activity of CuZnSOD suggested that ROS production was decreased in either cytosol or intermembrane space of mitochondria, which led us to further investigate the origin of ROS between control flies and $S_{O2}A$ flies.

Role of Mitochondria in Hyperoxia Tolerance

ROS production in mitochondria is believed to be a major source of ROS in cells. Therefore, we focused on the role of mitochondria in hyperoxia-induced oxidative stress by comparing control flies and $S_{O2}A$ flies. We first isolated mitochondria from fly thoraces and then determined the superoxide yield using electron paramagnetic resonance (EPR) techniques. A representative EPR curve was shown in Figure 4A and B and data were summarized in Figure 4C. Superoxide production was significantly decreased in mitochondria from $S_{O2}A$ flies as compared to those from control flies during state 3 respiration (Fig. 4C, $p < 0.05$) and a tendency of such a decrease was observed during state 4 respiration (Fig. 4C, $p = 0.07$). Previous studies have reported that

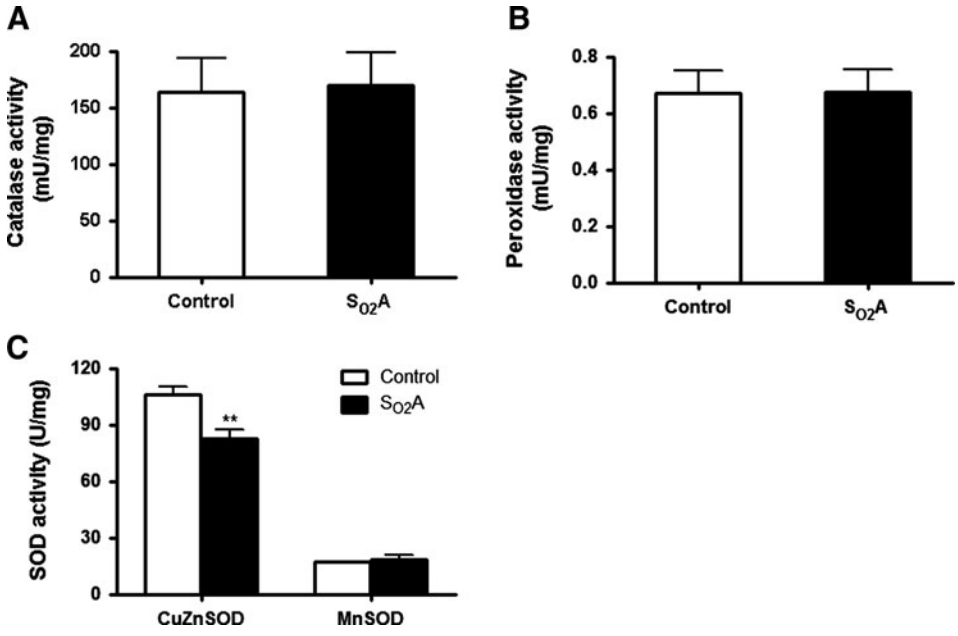

FIG. 3. Similar antioxidant enzyme activities between control and $S_{O2}A$ flies. Antioxidant enzyme activities were compared between control flies and $S_{O2}A$ flies. No difference was observed in the activities of **(A)** catalase, **(B)** peroxidase, and **(C)** manganese superoxide dismutase (MnSOD) between two groups except that a significantly decreased copper and zinc SOD (CuZnSOD) activity was observed in $S_{O2}A$ flies ($p < 0.01$). $^{**}p < 0.01$.

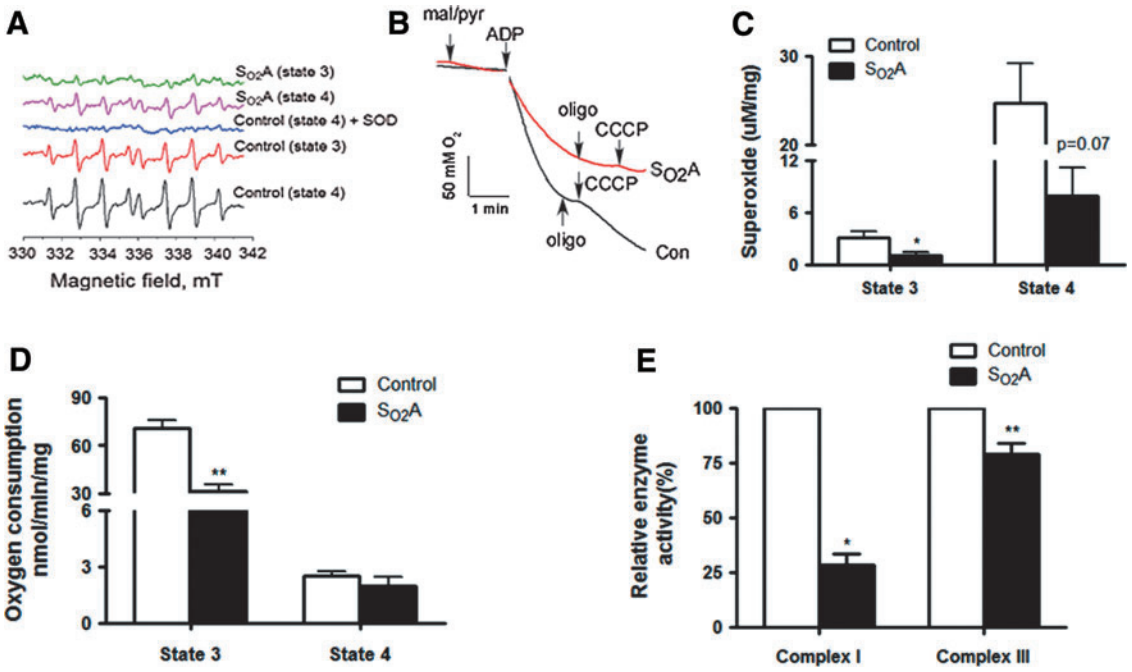

FIG. 4. Modification of mitochondrial functions in $S_{O2}A$ flies. Mitochondria from fly thoraces were isolated and the superoxide yield was determined using electron paramagnetic resonance (EPR) techniques. A representative EPR curve was shown in **(A)** and **(B)**. **(C)** Superoxide production was significantly decreased in mitochondria from $S_{O2}A$ flies as compared to those from control flies in state 3 respiration ($p<0.05$) and a tendency of such a decrease was observed in state 4 respiration ($p=0.07$). **(D)** Oxygen consumption in isolated mitochondria was compared and $S_{O2}A$ flies exhibited a significantly decreased state 3 respiration ($p<0.01$) as compared to control flies. **(E)** Enzymatic assay in isolated mitochondria revealed that $S_{O2}A$ flies exhibit a significantly decreased complex I ($p<0.05$) and complex III ($p<0.01$) activity than control flies. *$p<0.05$ and **$p<0.01$. (To see this illustration in color the reader is referred to the web version of this article at www.liebertonline.com/ars).

respiration-deficient (ρ°) HeLa cells exhibited significantly better growth rate and viability during exposure to 80% O_2 compared with wild-type counterparts, which was accompanied by reducing production of ROS from ETC in ρ° HeLa cells compared with control cells. A decreased superoxide yield was observed in isolated mitochondria from $S_{O2}A$ flies as compared to control flies, suggesting that decreased mitochondrial release of ROS might be an adaptive mechanism allowing $S_{O2}A$ flies to survive better in hyperoxia.

We also examined oxygen consumption in isolated mitochondria from both groups. As shown in Figure 4D, $S_{O2}A$ flies significantly decreased their mitochondrial oxidative phosphorylation during state 3 respiration ($p<0.01$) as compared to control flies, suggesting that $S_{O2}A$ flies have adapted to hyperoxic stress by decreasing ROS production in conjunction with decreasing O_2 consumption. No difference was seen between the two groups during resting respiration (state 4).

To explore the potential role of ETC individual complexes in decreased ROS production, we measured enzyme activities of ETC complex I and complex III, which are believed to be important in ROS leakage. In isolated mitochondria obtained from control flies and $S_{O2}A$ flies, we found that the enzyme activity of both complex I (Fig. 4E, $p<0.05$) and complex III (Fig. 4E, $p<0.01$) was significantly decreased in $S_{O2}A$ flies as compared to that in control flies. Inhibited ETC complex activity has been shown to increase ROS production, induce cellular injury, and activate programmed cell death. However, modulation of mitochondrial metabolism and ETC complex activity can be beneficial in settings such as ischemia or early reperfusion (3, 6, 7). Chen *et al.* have demonstrated that the reversible blockade of ETC with amobarbital, an inhibitor at the rotenone site of complex I, during ischemia protects mitochondria against ischemic damage by attenuating the mitochondrial release of ROS, enhancing contractile recovery, and decreasing myocardial infarct size (3). Szczepanek *et al.* demonstrated that transgenic mice, with cardiomyocyte-specific overexpression of mitochondria-targeted signal transducer and activator of transcription 3 (STAT3) with a mutation in the DNA-binding domain, are protected against ischemic injury in hearts by a STAT3-dependent partial blockade of ETC complex I activity and a decreased ROS production in mitochondria. One of their speculations is that the site of STAT3 interaction with complex I may be located proximal to the Fe/S N2 cluster, providing a site of relative blockade within complex I immediately before the likely site of ROS production (7). Similar phenomena were observed by Guzy *et al.* in a yeast study and they found that loss of complex III function in strains deficient in mitochondrial DNA (rho0) and the Rieske iron–sulfur protein in complex III abrogates the hypoxia-induced increase in ROS (5). The active modification of complex activity is also believed to be one of the protective mechanisms for tolerance in hibernating animals (1). Here, we observed that isolated mitochondria from $S_{O2}A$ flies exhibit a decreased complex I and III activity and a decreased ROS production. Therefore, we hypothesize that decreased complex activity results in a decreased ROS

production and that the site of inhibition in complex I and III as well as other factors such as ETC complex mutation or protein modification might play an important role in regulating complex activity.

In summary, we have shown that S_{O2}A flies exhibited a significantly longer lifespan under hyperoxia and paraquat-induced oxidative stress and these flies did not show an increased ROS production and increased oxidative stress markers as compared to control flies. A decreased ROS production, O_2 consumption, and a decreased ETC complex I and III activity were also observed in isolated mitochondria from S_{O2}A flies. We hypothesize that hyperoxia selection causes adaptive alteration of mitochondrial ETC complex activity leading to a reduction of superoxide production.

Notes

S_{O2}A flies and phenotypic assays

Hyperoxia-selected flies are generated through a long-term experimental selection and phenotypic assays are performed as described previously. In brief, for hyperoxia treatment, 3–5-day-old adult flies were exposed to 90% O_2 and the percent survival was scored daily; for paraquat treatment, 3–5-day-old flies were starved for 1 h and then transferred to vials, each containing two 1.5-cm circles of filter paper that had been soaked with 0.1 ml of 15 m*M* paraquat (methyl viologen; Sigma-Aldrich, St. Louis, MO), which was freshly prepared in 5% sucrose. The percent survival was scored every 8 and 16 h. Fresh paraquat solution was added every 24 h. Experiments were repeated at least four times for each line.

H_2O_2 determination, lipid peroxidation, and protein oxidation

Adult flies were homogenized and protein concentration was determined using a Bio-Rad protein assay kit (Bio-Rad, Hercules, CA). H_2O_2 production was measured with an Amplex Red H_2O_2/peroxidase assay kit (Invitrogen, Carlsbad, CA) according to the manufacturer's instructions.

MDA, an indicator of lipid peroxidation, was determined by LPO-586 assay kit (Oxis International, Inc., Foster City, CA). In brief, polyunsaturated fatty acid peroxides generate MDA upon decomposition, the decomposed MDA reacts with a chromogenic reagent, N-methyl-2-phenylindole, at 45°C, forms a stable chromophore, and yields a maximal absorbance at 586 nm.

Protein carbonyl content, as a marker of protein oxidation, was determined with the OxyBlot kit (Millipore, Billerica, MA) according to the manufacturer's recommendations. In brief, carbonyl groups in the protein side chains are derivatized to DNP, which can be further detected with rabbit anti-DNP antibody. Equal loading was assessed using an antibody against mouse polyclonal anti-β-actin (Sigma-Aldrich).

Antioxidant enzyme activities

SOD, catalase, and peroxidase activities were determined by SOD determination kit (Sigma-Aldrich), Amplex Red catalase assay kit, and Amplex Red H_2O_2/peroxidase assay kit (Invitrogen), respectively, following the standard protocol as recommended by manufactures. All assays were repeated at least three times.

Isolation of mitochondria from fly thorax

Mitochondria were isolated from thoracic muscle as previously described with minor modifications. Briefly, groups of 150 male flies were used per preparation. Live flies were chilled briefly on ice and thoraxes are dissected from the heads and abdomens under microscope. Isolated thoraces were placed in a chilled mortar, containing 300 μl of ice-cold isolation buffer (0.32 *M* sucrose, 10 m*M* EDTA, 10 m*M* Tris-HCl, and 2% bovine serum albumin, pH 7.3). The thoraxes were pounded gently without shearing to release mitochondria, and the preparation was maintained at 0°C–5°C throughout subsequent washing and centrifugation procedures. The debris was filtered through Spectra/Mesh nylon (10 μm pore size), and the volume was raised to 1.5 ml by washing the nylon membrane with additional isolation buffer. After centrifugation for 2 min at 250 *g*, the supernatant was transferred to a new tube and centrifuged for 10 min at 2200 *g*. The pellet was rinsed briefly in bovine serum albumin (BSA)-free isolation buffer, and then resuspended in 1.5 ml of the BSA-free buffer and centrifuged again. The mitochondrial pellet was resuspended in 300 μl of BSA-free isolation buffer for further analysis.

Mitochondrial functions

Oxygen consumption. Oxygen consumption was measured using a Clark-type oxygen electrode (Oxygraph™; Hansatech, Norfolk, United Kingdom). Purified mitochondria from *Drosophila* thoraxes ($\sim$100–200 μg protein) were added to the oxymetry chamber in a 300 μl solution containing 100 m*M* KCl, 75 m*M* mannitol, 25 m*M* sucrose, 5 m*M* H_3PO_4, 0.05 m*M* EDTA, and 10 m*M* Tris-HCl, pH 7.4. After 2-min equilibration, 5 m*M* pyruvate (pyr) and 5 m*M* malate (mal) were added and oxygen consumption was measured for 2 min. ADP (250 μM) was added to measure state 3 (phosphorylating) respiration. Oligomycin (oligo, 2.5 μg/ml) was added 2 min later to inhibit the F_0F_1-ATPase and determine state 4 (resting) respiration. The maximal uncoupled respiratory rate was obtained by adding 0.2 μM carbonyl cyanide m-chlorophenyl hydrazone (CCCP) to the mixture. Oxygen utilization traces and rate determinations were obtained using Oxygraph software.

Mitochondrial ROS generation using EPR analysis. Immediately after mixing mitochondria (0.1–0.2 mg of protein) with 70 m*M* 5-(diisopropoxyphosphoryl)-5-methyl-1-pyrroline-N-oxide (DIPPMPO) and appropriate combinations of the substrates, the mixture was loaded into 50-μl glass capillary and introduced into the EPR cavity of a MiniScope MS200 Benchtop spectrometer maintained at 37°C. We confirmed that the detected EPR signals are substrate specific, and not due to redox cycling in the studied mixtures, by lack of signals when DIPPMPO was mixed with combinations of substrates and inhibitors in the absence of mitochondria. EPR signals that accumulated over 10 min after mixing with substrates were quantified. Assignment of the observed signals from mitochondria is confirmed through computer-assisted spectral simulation using the WinSim software (http://epr.niehs.nih.gov/pest.html) and published spin parameters. EPR signal amplitudes were quantified and normalized with total mitochondrial protein concentration.

Mitochondrial ETC complex activity. Activities of complex I and III were measured following previous published protocols with minor modifications. In brief, the mitochondrial samples were suspended in 25 m*M* potassium phosphate buffer/5 m*M* $MgCl_2$ (pH 7.2) and then subjected to three rounds of freeze/thaw. The reaction mix for complex I activity included 2 m*M* KCN, 2 μg/ml antimycin A, 2.5 mg/ml BSA, 65 μM ubiquinone1, $\pm$ 2 μg/ml rotenone in 25 m*M* potassium phosphate buffer, and 5 m*M* $MgCl_2$ (pH 7.2). The complex I activity (NADH:ubiquinone oxidoreductase) was measured after adding 50 μg of mitochondrial sample and 0.13 m*M* NADH to the reaction mix and following a decrease in absorbance at 340 nm (with reference wavelength at 425 nm). The reaction mix for complex III activity contains 1 m*M* n-dodecylmaltoside, 1 m*M* KCN, 1 μg/ml rotenone, and 0.1% BSA in 50 m*M* potassium phosphate buffer (pH 7.4). The activity of complex III (cytochrome c reductase) was measured after adding 100 μM reduced decylubiquinone (DB.H2), 15 μM oxidized cytochrome c, and 30 μg of mitochondrial protein to the reaction mix and following an increase in absorbance at 550 nm. Each complex activity was presented after normalization to controls.

Statistics

Kaplan–Meier survival analysis was used to compare lifespan between groups; all other data were analyzed using Student's *t*-test or one-way ANOVA and graphed using GraphPad Prism 4.02 (GraphPad Software, Inc., San Diego, CA). Results were averaged from three individual replicates ($n = 3$) for each group and data were expressed as group mean $\pm$ SEM. Difference in means were considered statistically significant when $p < 0.05$.

Acknowledgments

Supported by NIH Grants RO1NS037756 and PO1HD032573 to Gabriel G. Haddad.

References

1. Brown JC, Chung DJ, Belgrave KR, and Staples JF. Mitochondrial metabolic suppression and reactive oxygen species production in liver and skeletal muscle of hibernating thirteen-lined ground squirrels. *Am J Physiol Regul Integr Comp Physiol* 302: R15–R28, 2012.
2. Campian JL, Qian M, Gao X, and Eaton JW. Oxygen tolerance and coupling of mitochondrial electron transport. *J Biol Chem* 279: 46580–46587, 2004.
3. Chen Q, Moghaddas S, Hoppel CL, and Lesnefsky EJ. Reversible blockade of electron transport during ischemia protects mitochondria and decreases myocardial injury following reperfusion. *J Pharmacol Exp Ther* 319: 1405–1412, 2006.
4. Clerch LB and Massaro D. Tolerance of rats to hyperoxia. lung antioxidant enzyme gene expression. *J Clin Invest* 91: 499–508, 1993.
5. Guzy RD, Mack MM, and Schumacker PT. Mitochondrial complex III is required for hypoxia-induced ROS production and gene transcription in yeast. *Antioxid Redox Signal* 9: 1317–1328, 2007.
6. Park JW, Chun YS, Kim YH, Kim CH, and Kim MS. Ischemic preconditioning reduces Op6 generation and prevents respiratory impairment in the mitochondria of post-ischemic reperfused heart of rat. *Life Sci* 60: 2207–2219, 1997.
7. Szczepanek K, Chen Q, Derecka M, Salloum FN, Zhang Q, Szelag M, Cichy J, Kukreja RC, Dulak J, Lesnefsky EJ, and Larner AC. Mitochondrial-targeted Signal transducer and activator of transcription 3 (STAT3) protects against ischemia-induced changes in the electron transport chain and the generation of reactive oxygen species. *J Biol Chem* 286: 29610–29620, 2011.
8. Zhao HW, Zhou D, and Haddad GG. Antimicrobial peptides increase tolerance to oxidant stress in *Drosophila melanogaster*. *J Biol Chem* 286: 6211–6218, 2011.
9. Zhao HW, Zhou D, Nizet V, and Haddad GG. Experimental selection for *Drosophila* survival in extremely high O2 environments. *PLoS One* 5: e11701, 2010.

Address correspondence to:
Dr. Gabriel G. Haddad
Department of Pediatrics
University of California–San Diego
9500 Gilman Drive
La Jolla, CA 92093-0735

E-mail: ghaddad@ucsd.edu

Dr. Sameh S. Ali
Department of Medicine and Anesthesiology
University of California–San Diego
3350 La Jolla Village Drive
San Diego, CA 92161-9125

E-mail: ssali@ucsd.edu

Date of first submission to ARS Central, December 29, 2011; date of acceptance, January 2, 2012.

Abbreviations Used

BSA = bovine serum albumin
CCCP = carbonyl cyanide m-chlorophenyl hydrazone
CuZnSOD = copper and zinc superoxide dismutase
DB.H2 = reduced decylubiquinone
DIPPMPO = 5-(diisopropoxyphosphoryl)-5-methyl-1-pyrroline-N-oxide
DNA = deoxyribonucleic acid
DNP = 2,4-dinitrophenylhydrazine
EPR = electron paramagnetic resonance
ETC = electron transport chain
H_2O_2 = hydrogen peroxide
MDA = malonaldehyde
MnSOD = manganese superoxide dismutase
ROS = reactive oxygen species
$S_{O2}A$ = hyperoxia selected
STAT3 = signal transducer and activator of transcription 3